Received: 29 November 2019 | Revised: 27 December 2019 | Accepted: 27 January 2020

DOI: 10.1002/chir.23186

WILEY

SPECIAL ISSUE ARTICLE

Design and synthesis of chiral spirobifluorenes

Ani Ozcelik[1] | **María de los Ángeles Peña-Gallego**[2] | **Raquel Pereira-Cameselle**[1] | **J. Lorenzo Alonso-Gómez**[1]

[1]Departamento de Química Orgánica, Universidad de Vigo, Vigo, Spain

[2]Departamento de Química Física, Universidad de Vigo, Vigo, Spain

Correspondence
Raquel Pereira-Cameselle and Lorenzo Alonso-Gómez Departamento de Química Orgánica, Universidad de Vigo, Campus Universitario, E-36310 Vigo, Spain.
Email: raquel@uvigo.es; lorenzo@uvigo.es

Funding information
IBEROS, Grant/Award Number: 0245_IBEROS_1_E; Xunta de Galicia, Grant/Award Numbers: GRC2019/24, ED431F 2016/005

Abstract

Chiroptical spectroscopic methods serve as a practical tool for the structural characterization of chiral systems based on the interaction with polarized light. The higher sensitivity of these methods, compared with their achiral counterparts, not only enables the determination of absolute configuration and conformational preferences, but also supramolecular interactions may be monitored. In order to expand the applicability of chiroptical systems, the development of functional materials exhibiting intense chiroptical responses is essential. As a proof of principle, we previously constructed chiroptical interfaces via thioacetate-derivatized allenes. Because of the photoisomerization issues associated with allenes, we have recently proposed their replacement by spirobifluorenes to achieve robust chiroptical systems. Thus, we hereby present the design and synthesis of chiral spirobifluorenes bearing thioacetates suitable for suface functionalization.

KEYWORDS

chiroptical responses, enantiomeric resolution, spriobifluorenes, synthesis

1 | INTRODUCTION

Objects are said to be chiral when they do not coincide with their mirror images. This property is prevalent in nature where the building blocks of life, ie, amino acids or sugars, are chiral.[1,2] Particularly, left- and right-handed molecules are referred to as enantiomers and they uniquely respond to another chiral entity. Likewise, chiroptical responses arise when enantiomeric forms interact with circularly polarized light that could feature two opposite handedness.[3,4] Based on this fact, chiroptical spectroscopies such as electronic and vibrational circular dichroism (ECD and VCD) or optical rotatory dispersion (ORD) are routinely employed to explore chiral systems.[5] Unlike conventional ultraviolet-visible (UV/Vis) and fluorescence spectroscopies, chiroptical methods are highly sensitive to predict absolute configuration (AC)[6,7] and conformational preferences.[8,9] Additionally, from short to long-range supramolecular interactions may be monitored as long as any chiral component is present.[10,11]

The advantages of chiroptical responses could be also beneficial for applications besides structure elucidation. Nevertheless, suitable chiroptical systems are scarce. Great effort has been accordingly devoted to the development of systems involving purely organic molecules,[12] complexes,[13,14] or plasmonic nanostructures[15,16] with remarkable chiroptical properties in solution. In this regard, we have achieved oligomeric,[17] cyclic,[18] or cage-shaped[19] molecular geometries through axially chiral allenes. From the application point of view, the efficient integration of chiroptical systems into devices is fundamental and hence the state of matter must be carefully chosen to meet the requirements of a specific application. Whereas chiroptical solutions are by far the most abundant, little is known regarding the construction of two-dimensional (2D) chiroptical surfaces that could be employed in daily life. Among other strategies,[20] the

inherent chirality of small organic molecules could be bestowed upon metal surfaces by self-assembly.[21,22] To this end, we employed chiral framework (CF) **CF-1** bearing allenes on Ag (111) under vacuum conditions (Figure 1A). While the molecular chirality was transferred to 2D nanostructures by the formation of up-standing chiral architectures (UCAs), the poor stability of these first examples hindered the exploration of chiroptical responses at room temperature.[23] To tackle this challenge, we undertook the strategy of self-assembled monolayers (SAMs)[24] and synthesized both enantiomers of thioacetate-derivatized **CF-2** for the functionalization of Au surfaces (Figure 1B). Remarkably, the chiroptical responses of the formed nanoarchitectures were addressed by means of second harmonic generation CD spectroscopy on a custom-made transparent substrate.[21] However, allenes may undergo photoisomerization,[8,25] limiting their exploitation for everyday applications.

For the last two decades, there has been a rapid rise in the use of spirobifluorenes (SBFs) in the field of organic electronics due to their high rigidity, solubility, and peculiar electronic properties provided by the orthogonal arrangement of two fluorine units connected by a shared quaternary atom.[26-28] Furthermore, such compounds may feature axial chirality upon appropriate substitution. In comparison with different positional isomers, 2-substituted SBFs are particularly available for the extension of conjugation, leading to tuning optical properties in a well-controlled fashion.[29] Seeking for a more robust chiral axis, we have theoretically[30] and experimentally[31] evaluated the reliability of SBFs in the construction of stable systems presenting remarkable

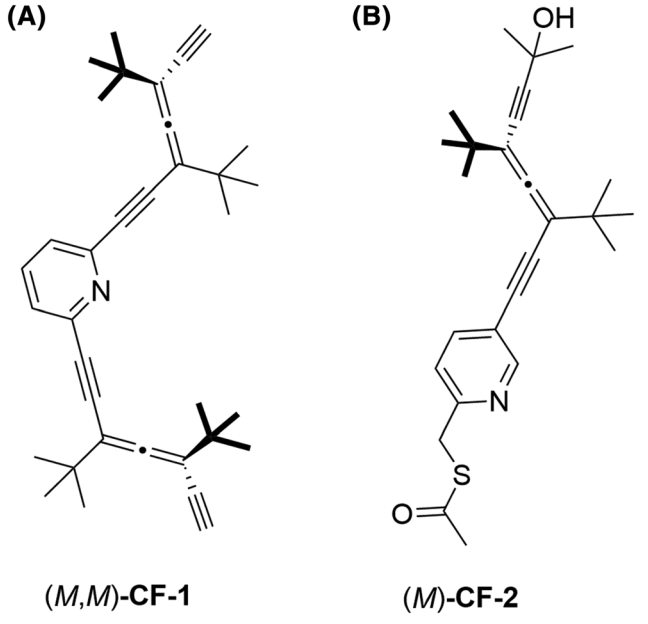

FIGURE 1 Structures of (A) (*M*,*M*)-**CF-1** and (B) (*M*)-**CF-2** previously studied for surface functionalization[21,23]

chiroptical responses in solution. Consequently, we herein report the design, synthesis, and AC assignment of thioacetate functionalized SBFs **CF-3**, **CF-4**, and **CF-5** as a milestone towards the development of chiroptical surfaces (Scheme 1).

2 | MATERIALS AND METHODS

2.1 | General methods

Solvents were dried according to published methods and distilled before use.[32] high-performance liquid chromatography (HPLC)–grade solvents were used for the HPLC purification. All other reagents were commercial compounds of the highest purity available. Unless otherwise stated, all reactions were performed under nitrogen atmosphere. Flash column chromatography (FC) was carried out using Merck Kieselgel 60 (230-400 mesh) under pressure. Analytical thin layer chromatography (TLC) was performed on aluminum plates with silica gel Macherey-Nagel UV254 and visualized by UV irradiation (254 nm) or 365 nm or by staining with a solution of phosphomolybdic acid. HPLC was performed using the separations module Waters 2695, the photoiode array detector Waters 996, and the chiral stationary phase Chiralpak IA (Diacel Chemical Industries Ltd.). UV/Vis and ECD spectra were recorded on a Jasco J-815 spectropolarimeter at 25°C employing 1 cm cuvette. ^{1}H NMR and ^{13}C NMR spectra were recorded in $CDCl_3$ at 25°C on a Bruker AMX-400 spectrometer operating at 400.16 MHz and 100.62 MHz with residual protic solvent as the internal references ($CDCl_3$, ^{1}H = 7.26 ppm) for the former and (^{13}C = 77.16 ppm) for the latter.[33] Chemical shifts (δ) are given in parts per million (ppm), and coupling constants (J) are given in Hertz (Hz). The spectra are reported as follows: δ (multiplicity, coupling constant J, number of protons, and assignment). HRMS (ESI^+) were measured with an APEX3 instrument. All computational calculations were carried out using the Gaussian 09[34] program package.

2.2 | General procedure for copper-free Sonogashira couplings of terminal spiranic alkyne

Spiranic alkyne (1 eq), aryl or heteroaryl bromide (1.2-1.5 eq), Pd $(PPh_3)_4$ (0.1 eq), Et_3N (8.0 eq), and DMF were added to a heat-gun-dried Schlenk tube. The resulting mixture was thoroughly degassed with three freeze-thaw cycles and stirred for 20 h at 100°C. After allowing to cool down to room temperature, the crude

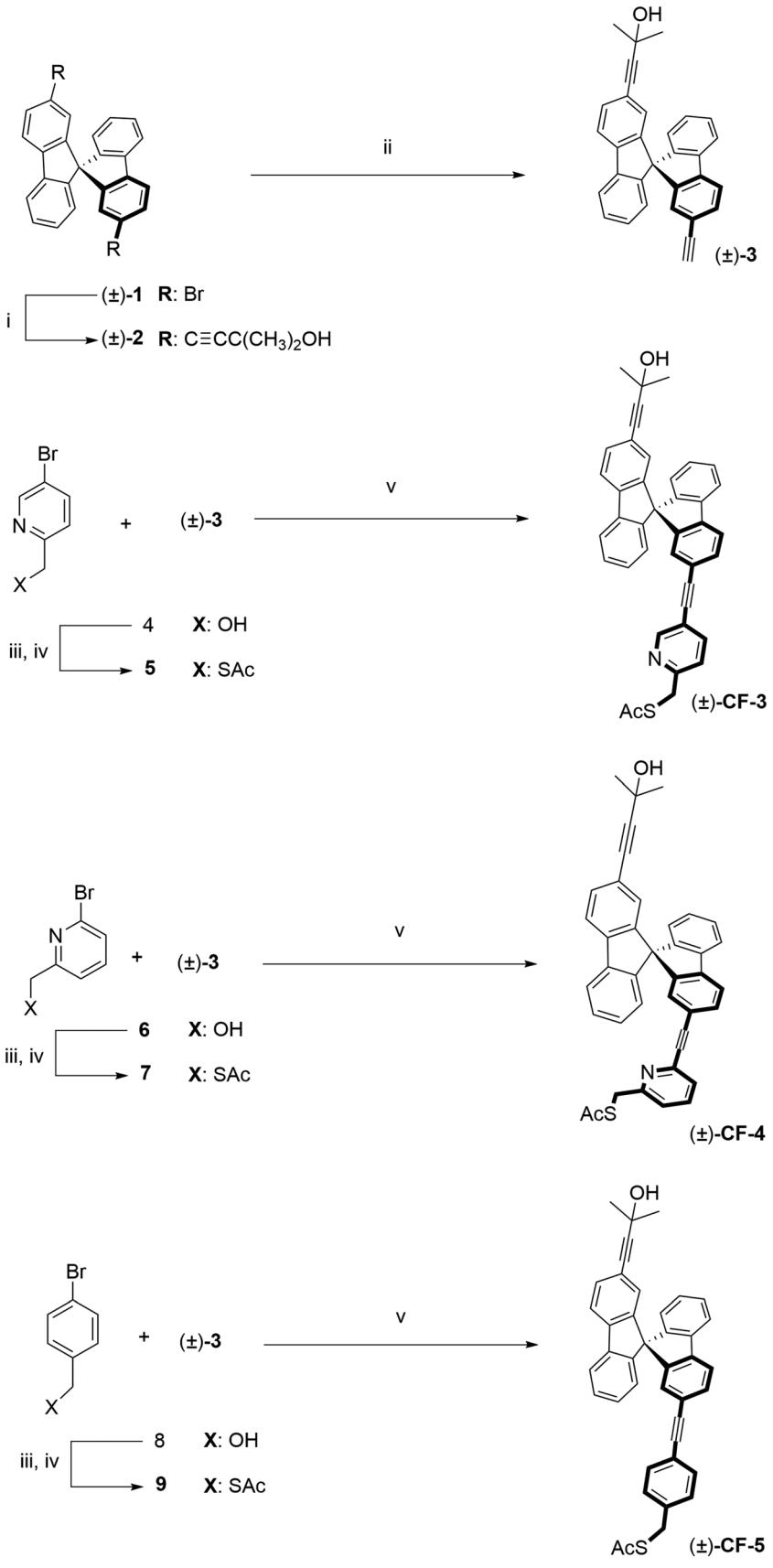

SCHEME 1 Synthesis of chiral frameworks. Reagents and conditions: (i) 2-methyl-3-butyn-2-ol Pd $(PPh_3)_4$, Et_3N, DMF, 24 h, 71%; (ii) NaOH, Toluene, 90°C, 8 h 78%; (iii) $MeSO_2Cl$, Et_3N, CH_2Cl_2, 0-25°C, 20-24 h; (iv) KSAc, DMF, 0-25°C, 3 d, 80% (**5**), 69% (**7**), and 73% (**9**); (v) Pd $(PPh_3)_4$, Et_3N, DMF, 20 h, 47% ((±)-**CF**-**3**), 66% ((±)-**CF**-**4**), and 24% ((±)-**CF**-**5**). For the sake of simplicity, acetyl group is abbreviated as Ac

was extracted with CH_2Cl_2 (3×), washed with deionized water (3×) and brine (3×), and dried over anhydrous Na_2SO_4.

2.3 | General procedure for preparation of thioacetates

Into a heat-gun-dried round-bottom flask, alcohol (1.0 eq) was dissolved in CH_2Cl_2 and cooled to 0°C. Subsequently, Et_3N (1.5 eq) and $MeSO_2Cl$ (2.0 eq) were added dropwise. After 10 minutes, the ice bath was removed and the resulting mixture was stirred for 18 to 24 hours at 25°C. Once the reaction was completed, an aqueous solution of saturated $NaHCO_3$ was added. The reaction mixture was extracted with CH_2Cl_2 (3×), washed with deionized water (2×) and brine (1×), and dried over anhydrous Na_2SO_4. The resulting oil was dissolved in DMF and cooled to 0°C. After addition of KSAc (1.5 eq), the ice bath was removed and the mixture was stirred for 3 days at 25°C. The crude was poured to deionized water and extracted with CH_2Cl_2 (3×). The organic layer was washed with deionized water (4×) and brine (2×) and dried over anhydrous Na_2SO_4. Finally, the solvent was evaporated under vacuum to give the corresponding thioacetate of sufficient purity.

2.3.1 | (±)-2,2′-bis(3-methyl-3-hydroxy-1-butyn-1-yl)-9,9′SBF((±)-2)

Into a heat-gun-dried Schlenk tube, (±)-2,2′-dibromo-9,9′-SBF ((±)-**1**) (1.05 mmol, 500 mg) and Pd $(PPh_3)_4$ (0.21 mmol, 243 mg) were added and purged for 10 minutes. Afterwards, Et_3N (5.3 mL) and DMF (15.7 mL) were added. The resulting mixture was purged for additional 30 minutes. Finally, 2-methyl-3-butyn-2-ol (5.27 mmol, 0.52 mL) was added and the mixture stirred for 24 hours at 105°C. After cooling down, the deionized water was added. The aqueous layer was extracted with CH_2Cl_2 (3×) and the organic layer washed with deionized water (4×) and brine (2×) and dried over anhydrous Na_2SO_4. Purification via flash column chromatography (SiO_2, 30% EtOAc/*n*-hexane) yielded (±)-**2** as pale brown solid (362.3 mg, 71%). ^{1}H NMR (400.16 MHz, $CDCl_3$, δ): 7.83 (d, J = 7.5 Hz, 2H, H5 and H5′), 7.78 (dd, J = 7.9, 0.7 Hz, 2H, H4 and H4′), 7.44 (dd, J = 7.9, 1.5, 2H, H3 and H3′), 7.38 (td, J = 7.5, 1.1 Hz, 2H, H6 and H6′), 7.13 (td, J = 7.5, 1.1 Hz, 2H, H7 and H7′), 6.77 (dd, J = 1.5, 0.7 Hz, 2H, H1 and H1′), 6.72 (d, J = 7.6 Hz, 2H, H8 and H8′), 1.51 (s, 12H, 2×$(CH_3)_2$) ppm. ^{13}C NMR (100.63 MHz, $CDCl_3$, δ): 148.6 (2×, C8b, and C8b′), 148.4 (2×, C8a, and C8a′), 142 (2×, C4a and C4a′), 141.2 (2×, C4b and C4b′), 131.7 (2×, C3 and C3′), 128.5 (2×, C6 and C6′), 128.2 (2×, C7 and C7′), 127.5 (2×, C1 and C1′), 124.3 (2×, C8 and C8′), 120.5 (2×, C4 and C4′), 120.1 (2×, C5 and C5′), 94.2 (2×, —C≡<u>C</u>C $(CH_3)_2OH$), 82.0 (2×, —<u>C</u>≡CC $(CH_3)_2OH$), 65.7 (2×, —<u>C</u> $(CH_3)_2OH$), 65.6 (C9), 31.5 (4×, —C(<u>C</u>$H_3)_2OH$) ppm. ESI-MS: m/z Calcd. for $C_{35}H_{28}NaO_2$ $[(M + Na)]^+$ 503.19815; found, 503.19816.

2.4 | (±)-2-(3-methyl-3-hydroxy-1-butyn-1-yl)-2′-ethynyl-9,9′-spirobi[fluorene]((±)-3)

(±)-**2** (0.47 mmol, 227 mg), anhydrous NaOH (70.5 mmol, 2834 mg), and dry toluene (94 mL) were added to the heat-gun-dried two-necked round-bottom flask. The mixture was stirred for 8 hours at 90°C. After cooling to room temperature, deionized water was added and the aqueous layer was extracted with EtOAc (3×). The organic layer was washed with deionized water (2×) and brine (1×) and dried over anhydrous Na_2SO_4. Purification via flash column chromatography (SiO_2, gradient from 25% to 30% EtOAc/*n*-hexane) gave (±)-**3** as pale yellow solid (155.0 mg, 78%). Spectroscopic data matched to that of previously reported.[31] ^{1}H NMR (400.16 MHz, $CDCl_3$, δ): 7.9 – 7.8 (m, 4H), 7.53 (dd, J = 7.9, 1.4 Hz, 1H), 7.45 (dd, J = 7.9, 1.4 Hz, 1 H), 7.39 (td, J = 7.5, 1.0 Hz, 1H), 7.38 (td, J = 7.5, 1.0 Hz, 1H), 7.14 (td, J = 7.5, 1.0 Hz, 1H), 7.13 (td, J = 7.5, 1.1 Hz, 1H), 6.84 (dd, J = 1.3, 0.5, 1H), 6.77 (dd, J = 1.4, 0.5, 1H), 6.73 (d, J = 7.6 Hz, 1H), 6.72 (d, J = 7.6 Hz, 1H), 2.97 (s, 1H, C≡C—H), 1.52 (s, 6H, 2×CH_3) ppm.

2.4.1 | 5-bromo-2-(acetylthiomethyl) pyridine (5)

Following the general procedure for the preparation of thioacetates, alcohol **4** (1.06 mmol, 200 mg) was dissolved in CH_2Cl_2 (2.9 mL) and treated with Et_3N (1.6 mmol, 0.22 mL) and $MeSO_2Cl$ (2.20 mmol, 0.12 mL) for 18 hours. After work-up, the crude was dissolved in DMF (5.3 mL) and stirred for 48 hours with KSAc (1.60 mmol, 182 mg) to give **5** as a pale brown oil (195 mg, 80%). The spectroscopic data was identical that of previously reported.[21] ^{1}H NMR (400.16 MHz, $CDCl_3$, δ): 8.58 (d, J = 1.9 Hz, 1H, C6), 7.74 (d, J = 8.3 Hz, 1H, Py), 7.26 (d, J = 8.3, 1H, Py), 4.19 (s, 2H, $PyCH_2S$), 2.36 (s, 3H, $SCOCH_3$) ppm.

2.4.2 | 6-bromo-2-(acetylthiomethyl) pyridine (7)

Following the general procedure for the preparation of thioacetates, alcohol **6** (1.06 mmol, 200 mg) was dissolved

in CH_2Cl_2 (2.9 mL) and treated with Et_3N (1.6 mmol, 0.22 mL) and $MeSO_2Cl$ (2.20 mmol, 0.12 mL) for 24 hours. After work-up, the crude was dissolved in DMF (6 mL) and stirred for 72 hours with KSAc (1.60 mmol, 182 mg) to give **7** as a pale brown oil (181 mg, 69%). ^{1}H NMR (400.16 MHz, $CDCl_3$, δ): 7.48 (t, J = 7.6 Hz, 1H), 7.35 (d, J = 7.6 Hz, 1H), 7.32 (d, J = 7.6 Hz, 1H), 4.20 (s, 2H, $PyCH_2S$), 2.35 (s, 2H, $SCOCH_3$) ppm. ^{13}C NMR (100.62 MHz, $CDCl_3$, δ): 194.5 (—**C**=O), 158.8 (C2, Py), 141.3 (C6, Py), 139.0 (C4, Py), 126.5 (C5, Py), 122.0 (C3, Py), 34.7 (Py**C**H_2S), 30.2 (SCO**C**H_3) ppm. ESI-MS: m/z Calcd. for $C_8H_9{}^{79}BrNOS$ and $C_8H_9{}^{81}BrNOS$ [(M + H)]+, 245.95827 and 247.95662; found, 245.95866 and 247.95662.

2.4.3 | 4-bromo-1-(acetylthiomethyl) benzene (9)

Following the general procedure for the preparation of thioacetates, alcohol **8** (2.67 mmol, 500 mg) was dissolved in CH_2Cl_2 (7.4 mL) and treated with Et_3N (4.00 mmol, 0.56 mL) and $MeSO_2Cl$ (5.35 mmol, 0.31 mL) for 22 hours. After work-up, the crude was dissolved in DMF (9.9 mL) and stirred with KSAc (4.00 mmol, 457 mg) to give **9** as a dark brown oil (475 mg, 73%). ^{1}H NMR (400.16 MHz, $CDCl_3$, δ): 7.41 (d, J = 8.5, 2H, H3 and H5), 7.16 (d, J = 8.5, 2H, H2 and H6), 4.05 (s, 2H, $PhCH_2S$), 2.34 (s, 3H, $SCOCH_3$) ppm. ^{13}C NMR (100.63 MHz, $CDCl_3$, δ): 194.9 (—**C**=O), 136.9 (C), 131.8 (2×, C3 and C5, Ph), 130.6 (2×, C2 and C6, Ph), 121.3 (C), 32.9 (Ph**C**H_2S), 30.4 (SCO**C**H_3) ppm. ESI-MS: m/z Calcd. for $C_9H_{10}{}^{79}BrOS$ and $C_9H_{10}{}^{81}BrOS$ $[(M + H)]^+$, 244.9630 and 246.9609; found, 244.9639 and 246.9620.

2.4.4 | (±)-2′-[(5-[(acetylthio)methyl] pyridin-2-yl)ethynyl]-2-(3-hydroxy-3-methylbut-1-yn-1-yl)-9,9′-spirobi[fluorene] ((±)-CF-3)

Following the general procedure described for copper-free Sonogashira cross-coupling, spiranic alkyne (±)-**3** (0.14, 60 mg), aryl bromide **5** (0.20 mmol, 48.2 mg), Pd $(PPh_3)_4$ (0.014 mmol,16.4 mg), Et_3N (1.12 mmol, 0.16 mL), and DMF (1.5 mL) were added to a heat-gun-dried Schlenk tube. After stirring the mixture up for 20 hours and work-up, purification of the crude through flash column chromatography (SiO_2, gradient from 25% to 40% EtOAc/*n*-hexane) yielded (±)-**CF-3** (38.8 mg, 47%) as pale yellow solid. ^{1}H NMR (400.16 MHz, $CDCl_3$, δ): 8.57 (dd, J = 2.1, 0.9 Hz, 1H, H6″), 7.9 – 7.8 (m, 3H, H5, H5′ and H4), 7.80 (d, J = 7.9 Hz, 1H, H4′), 7.63 (dd, J = 8.1, 2.1 Hz, 1H, H4″), 7.58 (dd, J = 7.9, 1.3 Hz, 1H, H3), 7.47 (dd, J = 7.9, 1.3 Hz, 1H, H3′), 7.42 (td, J = 7.5, 1.5 Hz, 1H, H6), 7.41 (td, J = 7.5, 1.5 Hz, 1H, H6′), 7.30 (d, J = 7.8 Hz, 1H, H3″), 7.17 (td, J = 7.6, 1.1 Hz, 1H, H7), 7.16 (td, J = 7.6, 1.1 Hz, 1H, H7′), 6.91 (d, J = 1.0 Hz, 1H, H1), 6.81 (d, J = 1.0 Hz, 1H, H1′),6.76 (d, J = 7.5 Hz, 1H, H8), 6.75 (d, J = 7.5 Hz, 1H, H8′), 4.24 (s, 2H, $PyCH_2S$), 2.37 (s, 3H, $SCOCH_3$), 1.53 (s, 6H, C $(CH3)_2$) ppm. ^{13}C NMR (100.63 MHz, $CDCl_3$, δ): 194.9(—**C**=O), 156.4 (C2″, Py), 151.7 (C6″, Py), 148.7, 148.6, 148.4, 148.2, 142.5, 141.9, 141.1, 141.0, 139.1 (C4″, Py), 131.8 (C3), 131.7 (C3′), 128.6 (C7), 128.5 (C7′), 128.2 (2×, C6 + C6′), 127.4 (2×, C1 + C1′), 124.3 (C8), 124.2 (C8′), 122.8 (C3″, Py), 122.1 (C2), 121.7 (C2′), 120.6, 120.5, 120.2, 120.1, 118.9 (C5″, Py), 94.4 (—**C**≡CC $(CH_3)_2OH$), 93.1 (—C≡**C**C $(CH_3)_2OH$), 86.3 (—**C**≡CPy), 82.3 (—C≡**C**Py), 65.6 (2×, C9 and **C** $(CH_3)_2OH$), 35.3 (Py**C**H_2S), 31.5 (2×C (**C**$H_3)_2OH$), 30.3 (—CO**C**H_3) ppm. HRMS-ESI: m/z Calcd. for $C_{40}H_{30}NO_2S$ $[(M + H)]^+$, 588.19918; found, 588.19843.

2.4.5 | (±)-2′-[(6-[(acetylthio)methyl] pyridin-2-yl)ethynyl]-2-(3-hydroxy-3-methylbut-1-yn-1-yl)-9,9′-spirobi[fluorene] ((±)-CF-4)

Following the general procedure described for copper-free Sonogashira cross-coupling, (±)-**3** (0.14, 60 mg), heteroaryl bromide **7** (0.17 mmol, 41.3 mg), Pd $(PPh_3)_4$ (0.014 mmol,16.4 mg), Et_3N (1.2 mmol, 0.16 mL), and DMF (1.5 mL) were added to a heat-gun-dried Schlenk tube. After stirring the mixture up for 20 hours and work-up, purification of the crude through flash column chromatography (SiO_2, 35% EtOAc/*n*-hexane) yielded (±)-**CF-4** as pale yellow solid (54.5 mg, 66%).^{1}H NMR (400.16 MHz, $CDCl_3$, δ): 7.9 – 7.8 (m, 3H, H5, H4 and H5′), 7.78 (d, J = 7.9 Hz, 1H, H4′), 7.62 (dd, J = 7.9, 1.5 Hz, 1H, H3), 7.53 (t, J = 7.8 Hz, 1H and H4″), 7.44 (dd, J = 7.9, 1.5 Hz, 1H, H3′), 7.40 (td, J = 7.5, 1.5 Hz, 1H and H6), 7.38 (td, J = 7.5, 1.5 Hz, 1H, H6′), 7.26 (d, J = 7.5 Hz, 1H, H5″), 7.23 (d, J = 7.5 Hz, 1H, H3″), 7.15 (td, J = 7.6, 1.1 Hz, 1H, H7), 7.13 (td, J = 7.6, 1.1 Hz, 1H, H7′), 6.96 (d, J = 1.2 Hz, 1H, H1), 6.82 (d, J = 1.1 Hz, 1H, H1′), 6.75 (d, J = 7.8 Hz, 1H, H8), 6.73 (d, J = 7.8 Hz, 1H, H8′), 4.25 (s, 2H, $PyCH_2S$), 2.33 (s, 3H, C OCH_3)0.1.51 (s, 6H, 2×C$(CH_3)_2$) ppm. ^{13}C NMR (100.63 MHz, $CDCl_3$, δ): 195.1 (—**C**=O), 158.2 (C2″, Py), 148.6, 148.5, 148.4, 148.2, 142.9 (C6″, Py), 142.6, 141.9, 141.1, 141.0, 137.0 (C4″, Py), 131.9 (C3), 131.7 (C3′), 128.7 (C7), 128.5 (C7′), 128.2 (2×, C6 and C6′), 128.1 (C1), 127.4 (C1′), 125.7 (C5″, Py), 124.3 (C8), 124.2(C8′), 122.5 (C3″, Py), 122.1 (C2′), 121.3 (C2), 120.6, 120.5, 120.2, 120.1, 94.3 (**C**≡CC $(CH_3)_2OH$), 89.7 (C≡**C**C $(CH_3)_2OH$), 89.0 (—C≡**C**Py), 82.4 (—**C**≡CPy), 65.6 (2×, C9 and **C** $(CH_3)_2OH$), 35.4 (Py**C**H_2S), 31.5 (2×,

—C ($\underline{C}H_3)_2OH$), 30.3 (—CO$\underline{C}H_3$) ppm. HRMS-ESI: m/z Calcd. for $C_{40}H_{29}NNaO_2S$ $[(M + Na)]^+$, 610.18112; found, 610.18085.

2.4.6 | (±)-2′-[(5-[(acetylthio)methyl] benzene-2-yl)ethynyl]-2-(3-hydroxy-3-methylbut-1-yn-1-yl)-9,9′-spirobi[fluorene] ((±)-CF-5)

Following the general procedure described for copper-free Sonogashira cross-coupling, (±)-**3** (0.11, 45 mg), aryl bromide **9** (0.15 mmol, 36.5 mg), Pd $(PPh_3)_4$ (0.011 mmol,12.7 mg), Et_3N (0.99 mmol, 0.12 mL), and DMF (1.5 mL) were added to a heat-gun-dried Schlenk tube. After stirring the mixture up for 20 hours and work-up, purification of the crude through flash column chromatography (SiO_2, gradient from 25% to 30% EtOAc/*n*-hexane) led to (±)-**CF-5** as pale pale yellow solid (15.5 mg, 24%).

(400.16 MHz, $CDCl_3$, δ): 7.9 – 7.8 (m, 3H, H5, H5′ and H4), 7.78 (dd, J = 7.9, 0.5 Hz, 1H, H4′), 7.55 (J = 7.9, 1.5 Hz, 1H, H3′), 7.44 (J = 7.9, 1.5 Hz, 1H, H3), 7.39 (td, J = 7.4, 1.0 Hz, 2H, H6 and H6′), 7.33 (d, J = 8.3 Hz, 2H, H3″ and H5″), 7.20 (d, J = 8.3 Hz, 2H, H2″ and H6″), 7.14 (td, J = 7.4, 1.0 Hz, 2H, H7 and H7′), 6.88 (dd, J = 1.5, 0.5 Hz, 1H, H1′), 6.80 (dd, J = 1.5, 0.5 Hz, 1H, H1), 6.75 (d, J = 7.4 Hz, 1H, H8 or H8′), 6.73 (d, J = 7.4 Hz, 1H, H8 or H8′), 4.08 (s, 2H, $PhCH_2S$), 2.34 (s, 3H, SC OCH_3), 1.51 (s, 6H, 2×C$(CH_3)_2$) ppm.^{13}C NMR (100.63 MHz, $CDCl_3$, δ): 195.1 (—$\underline{C}$═O), 148.7, 148.6, 148.5, 148.4, 142.1, 142.0, 141.2 (2×), 137.9 (C1″, Ph), 131.8 (C3″ and C5″, Ph), 131.7 (C3 and C3′), 128.9 (C2″ and C6″,Ph), 128.5 (2×, C7 and C7′), 128.2 (2×, C6 and C6′), 127.5 (C1′), 127.4 (C1), 124.3 (2×, C8 and C8′), 122.6 (C), 122.3 (C4″, Ph), 122.1, 120.5 (2×, C5 and C5′), 120.2 (C4), 120.1 (C4′), 94.2 (C≡$\underline{C}$C $(CH_3)_2OH$) , 90.0 (—$\underline{C}$≡CPh), 89.7 (—C≡$\underline{C}$Ph), 82.5 ($\underline{C}$≡CC $(CH_3)_2OH$), 65.7 (2×, C9, and $\underline{C}$ $(CH_3)_2OH$), 33.4 (Ph$\underline{C}H_2S$), 31.5 (2×, —C ($\underline{C}H_3)_2OH$), 30.5 (—CO$\underline{C}H_3$) ppm. HRMS-ESI: m/z Calcd. for $C_{41}H_{30}NaO_2S$ $[(M + Na)]^+$, 609.18587; found, 609.18748.

3 | RESULTS AND DISCUSSION

3.1 | Design

The stability of a chiral molecule-substrate pair plays a crucial role towards the development of robust chiroptical surfaces. Taking into account the strategy of SAMs, surface properties could be tailored in a well-controlled fashioned through the adsorption of organic thiols on Au surfaces either from liquid or gas phase. Among the other coinage metals, Au strongly interacts with S and presents several advantages for instance not having stable oxides at ambient conditions. Therefore, the proposed CFs **CF-3**, **CF-4**, and **CF-5** (Scheme 1, Figure 2) are composed of a chiral moiety, an aromatic spacer, and a head group (Figure 2).

Whereas the chirality of CFs is introduced by the photostable SBF, an acetyl protection is undertaken for the anchoring group in order to avoid by-products encountered with thiols (ie, formation of disulfides, Scheme 1). Starting off with **CF-3**, this first member is the spiro analogue of the previously studied **CF-2**.[21] Referring to our earlier studies, the interaction between molecules and the surface by the pyridine ring is expected to favor up-right orientation. To further unveil the influence of the aromatic spacer on the properties of the resulting functionalized surfaces, spiro compounds **CF-4** and **CF-5** feature different substitution pattern and aromatic spacer, respectively.

3.2 | Synthesis

CF-3, **CF-4**, and **CF-5** were synthesized through a non-enantioselective pathway (Scheme 1), followed by enantiomeric resolution (more details are given in the next section).

Sonogashira cross coupling of (±)-**1** with a large excess of 2-methyl-3-butyn-2-ol gave disubstiuted (±)-**2** (71%). The reaction was also performed through CuI/Pd $(PPh_3)_2Cl_2$ catalytic system and the yield decreased by 20% since Cu(I) salts could induce the dimerization of acetylene through Glaser-type oxidative homocoupling. To investigate the effect of the solvent, toluene was

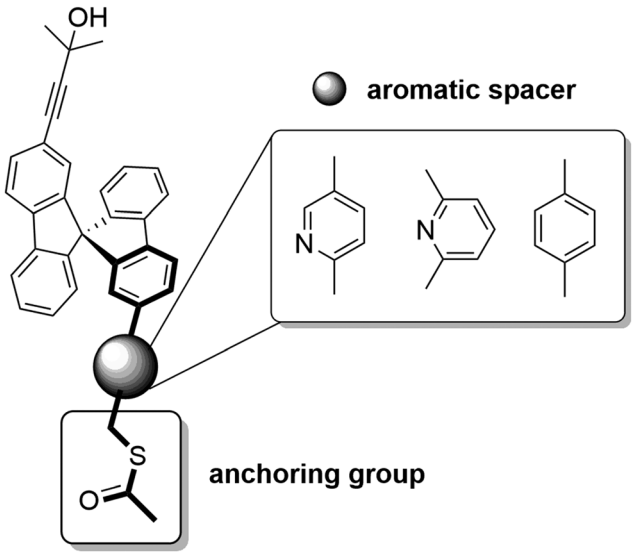

FIGURE 2 Representation of chiral frameworks

employed and no traces of product was observed. Subsequently, the selective deprotection was achieved by precisely controlling the reaction time as well as temperature leading to (±)-**3** in 78% yield. On the other hand, commercially available alcohols **4**, **6**, and **8** were transformed to the corresponding thioacetates by two consecutive S_N2 reactions. While the former involved the treatment of each alcohol with an excess of $MeSO_2Cl$ and Et_3N in CH_2Cl_2, the latter was the nucleophilic substitution of each mesylate by SAc in DMF, yielding **5** (80%), **7** (69%) and **9** (73%) of sufficient purity to be used without further purification. It is important to note that the described procedure for the preparation of each thioacetate was more efficient than Appel-type reaction conditions with CBr_4 and PPh_3. Finally, copper-free Sonogashira reaction between thioacetates **5**, **7**, and **9** with (±)-**3** afforded the desired CFs (±)-**CF-3** (47%), (±)-**CF-4** (66%), and (±)-**CF-5** (24%), respectively. Regarding the final step, the same conditions were employed to understand the reactivity of each aromatic halide. The higher yields for pyridine-containing CFs could be attributed to the inductive effect of the nitrogen atom, which is not present in thioacetate **9.**

TABLE 1 Thermal stability of **CF-3**, **CF-4**, and **CF-5**

Compound	Temperature (°C)
CF-3	**172.3**
CF-4	**254.5**
CF-5	**214.2**

TABLE 2 Enantiomeric resolution data of **CF-3**, **CF-4**, and **CF-5**

Compound	Solvent System	Flow (min/mL)	Retention Time (min)
CF-3	***i*-PrOH/CH_2Cl_2/*n*-Hex (2/20/78)**	**2.0**	**17.3[a]; 24.6[b]**
CF-4	***i*-PrOH/CH_2Cl_2/*n*-Hex (1/15/84)**	**2.0**	**35.0[a]; 39.5[b]**
CF-5	**Chloroform/*n*-Hex (30/70)**	**2.0**	**23.2[a]; 24.8[b]**

Abbreviation: HPLC, high-performance liquid chromatography.
[a]Retention times for fraction A obtained from HPLC.
[b]Retention times for fraction B obtained from HPLC.

The thermal bahavior of the racemic mixtures of **CF-3**, **CF-4**, and **CF-5** were examined by means of thermogravimetric analysis under air atmosphere. We note from Table 1 that overall the compounds presented high thermal stability, which may be affected by the substitution pattern as well as aromatic moiety. Once exceeding the presented temperature values, each compound was decomposed.

3.3 | Enantiomeric Resolution

The enantiomers of **CF-3**, **CF-4**, and **CF-5** were resolved through semi-preparative HPLC using the chiral stationary phase Chiralpak IA (CSP, Diacel Chemical Industries Ltd.). As summarized in Table 2, the conditions were slightly modified due to the different polarity of each compound (for chromtograms, see Supporting Information).

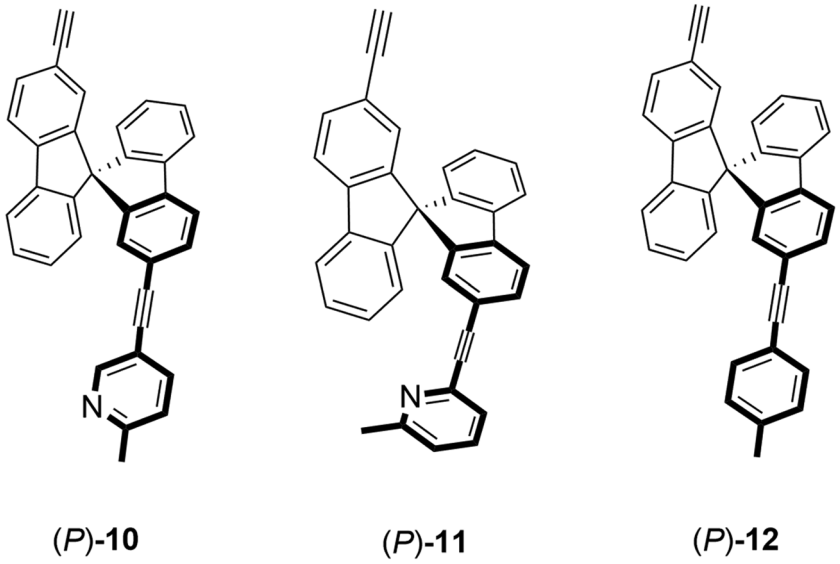

FIGURE 3 Simplified structures (*P*)-**10**, (*P*)-**11**, and (*P*)-**12** used for density functional theory (DFT) studies from **CF-3**, **CF-4**, and **CF-5**, respectively

3.4 | Absolute Configuration Assignment

Ab initio methods have been widely employed for shedding light on chiroptical responses.[35] Since our synthetic methodology was non-enantioselective, density functional theory (DFT) studies were carried out to unambigously assign the AC of each fraction obtained from the enantiomeric resolution.

The CFs were simplified by removing thioacetate and dimethyl alcohol moieties (Figure 3) due to the fact that their influence on the AC determination was found to be insignificant (for more details see Figures S1–S9 and S13–S15 in the Supporting Information). To perform conformational anaylses of simplified structures (*P*)-**10**, (*P*)-**11**, and (*P*)-**12**, the potential energy surfaces were initially scanned through varying dihedral angles in redundant coordinates at B3LYP/6-31G(d,p) (Figure 4). Unlike in the case of (*P*)-**12**, *anti* and *syn* conformations of similar energies were determined for pyridine bearing (*P*)-**10** and (*P*)-**11** as the N atom could be either in the vicinity or far from the spiranic C atom (Figure 4). Considering the experimental conditions and describing well the excited-state properties, the obtained geometries were further optimized and their vibrational frequencies were calculated at cam-B3LYP/6-31G(d,p) level including the solvent effect through the polarizable continuum model (PCM). ECD and UV/Vis spectra were subsequently simulated solving 20 states at the same level of theory. Typically, the chiral signatures of possible minima contribute in chiroptical responses as a function of their predicted Gibbs free energies according to Boltzmann distribution.[5] Therefore, ECD spectra of (*P*)-**11** and (*P*)-**12** were derived from the equal contribution of *anti* and *syn* conformations.

The experimental UV/Vis and ECD spectra were recorded for the resolved enantiomers of **CF-3**, **CF-4**, and **CF-5** in CH_2Cl_2 at different concentrations (from 2 ×

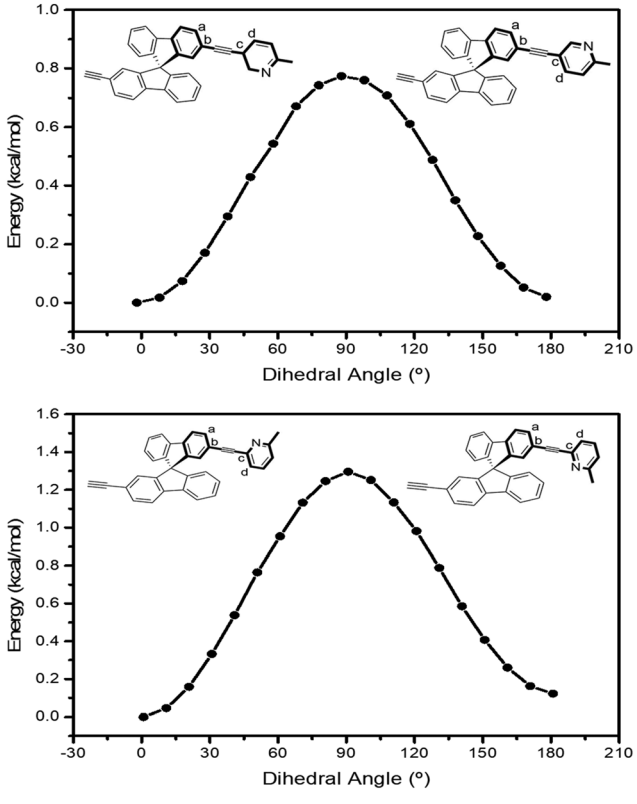

FIGURE 4 Conformational analyses of simplified structures (top) (*P*)-**10** and (bottom) (*P*)-**11** by potential energy surface mapping at B3LYP/6-31G(d,p) level. The dihedral angle is represented by a-b-c-d. The two minimum structures, *anti*- and *syn*-conformations, have similar energies

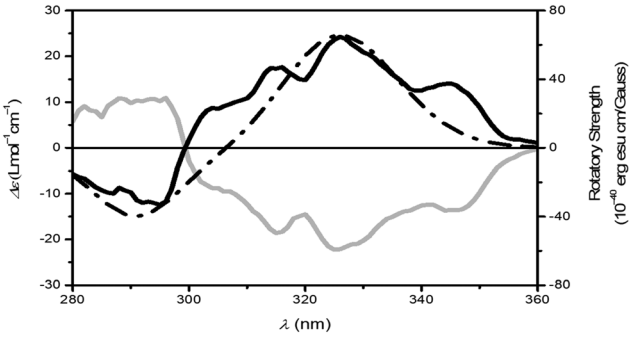

FIGURE 5 Comparison of the experimental circular dichroism (CD) spectra of the enantiomers of **CF-3** (solid grey and black lines for fractions A and B, respectively) with that of simulated of simplified structure (*P*)-**10** (dash dot line). The experimental spectra were measured in CH_2Cl_2 at a concentration of 2×10^{-5} M. For the sake of clarity, the simulated spectrum was shifted by 0.20 eV

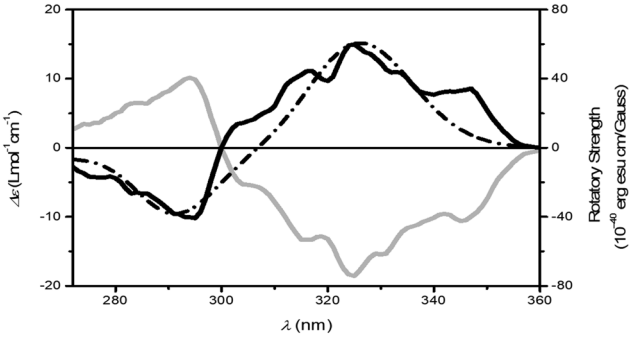

FIGURE 6 Comparison of the experimental circular dichroism (CD) spectra of the enantiomers of **CF-4** (solid grey and black lines for fractions A and B, respectively) with that of simulated of simplified structure (*P*)-**11** (dash dot line). The experimental spectra were measured in CH_2Cl_2 at a concentration of 4×10^{-5} M. For the sake of clarity, the simulated spectrum was shifted by 0.19 eV

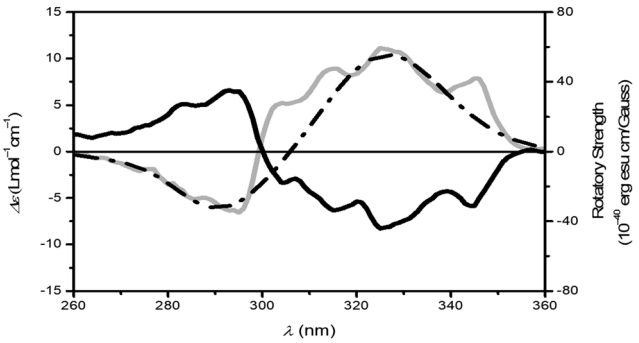

FIGURE 7 Comparison of the experimental circular dichroism (CD) spectra of the enantiomers of **CF-5** (solid grey and black lines for fractions A and B, respectively) with that of simulated of simplified structure (*P*)-**12** (grey solid line). The experimental spectra were measured in CH_2Cl_2 at a concentration of 4×10^{-5} M. For the sake of clarity, the simulated spectrum was shifted by 0.20 eV

10^{-5} M to 4×10^{-5} M). The prepared solutions were measured for 3 weeks under daylight irridiation. The characteristic shapes and intensities of the UV and ECD bands remained unchanged, demonstrating the photostability of the developed CFs (please refer to Figures S10–S12 in the Supporting Information for the spectra).

The experimental spectra feature vibronic couplings apart from the pure electronic transitions; however, they are broadly in a good agreement with the simulated ECD spectra of simplified structures (*P*)-**10**, (*P*)-**11**, and (*P*)-**12** (Figure 5–7). Whereas the lowest energy transition is located at 325 nm, the next is found at 296, 294, and 293 nm for the enantiomers of **CF-3**, **CF-4** and **CF-5**, respectively. Based on the comparison of the experimental and theoretically predicted ECD spectra, we can confidentially assign the fraction A for the enantiomeric resolution of **CF-3** and **CF-4** to (*P*). Regarding **CF-5**, the fraction A corresponds to (*M*) enantiomer.

4 | CONCLUSION

In summary, we have designed and synthesized highly stable thioacetate-derivatized SBFs **CF-3**, **CF-4**, and **CF-5** in 47%, 66%, and 24% yield, respectively. The subsequent enantiomeric resolution has been performed by means of HPLC with a CSP. On the other hand, ECD spectra have been simulated at the cam-B3LYP/6-31G(d,p) level of theory taking the solvent effect into account. The AC of each fraction obtained from HPLC has been unambiguously determined by direct comparison with the experimental ECD spectra of simplified structures (*P*)-**10**, (*P*)-**11**, and (*P*)-**12**. This work will not only give access to the functionalization of Au surfaces, but also it may lead to rationalizing the effect of substitution pattern as well as aromatic spacers on the chiroptical responses of the formed nanoarchitectures.

ACKNOWLEDGEMENTS

This work was funded by Xunta de Galicia (ED431F 2016/005 and GRC2019/24) and IBEROS (0245_IBEROS_1_E). A.O. thanks Xunta de Galicia for predoctoral fellowship. J.L.A.-G. thanks the Spanish Ministerio de Economía y Competividad for a "Ramón y Cajal" research contract. All authors gratefully acknowledge CACTI de Vigo. The authors also would like to thank A. Acuña Couña (CACTI de Vigo) for his support in the enantiomeric resolution and TGA analysis.

ORCID

Ani Ozcelik https://orcid.org/0000-0002-3475-6928
María de los Ángeles Peña-Gallego https://orcid.org/0000-0002-6898-8305
Raquel Pereira-Cameselle https://orcid.org/0000-0003-2634-9799
J. Lorenzo Alonso-Gómez https://orcid.org/0000-0002-6107-0120

REFERENCES

1. Gerlach H. Chirality: a relational geometric-physical property. *Chirality*. 2013;25(11):684-685.
2. Inaki M, Liu J, Matsuno K. *Philos Trans R Soc B Biol Sci*. 2016; 371:1-9.
3. Cid MM, Bravo J (Eds). Structure Elucidation in. Organic Chemistry: *The Search for the Right Tools*, Wiley, 2015.
4. Ernst KH. *Surf Interface Sci*. 2016;6:695-748.
5. Petrovic AG, Navarro-Vázquez A, Alonso-Gómez JL. *Curr Org Chem*. 2010;14:1612-1628.
6. Alonso-Gómez JL, Schanen P, Rivera-Fuentes P, Seiler P, Diederich F. 1,3-Diethynylallenes (DEAs): enantioselective synthesis, absolute configuration, and chiral induction in 1,1,4,4-tetracyanobuta-1,3-dienes (TCBDs). *Chem A Eur J*. 2008;14(34):10564-10568.
7. Li D, Hu R, Guo D, et al. *J. Phys. Chem C*. 2017;121:20947-20954.
8. Alonso-Gómez JL, Petrovic AG, Harada N, Rivera-Fuentes P, Berova N, Diederich F. Chiral induction from allenes into twisted 1,1,4,4-tetracyanobuta-1,3-dienes (TCBDs): conformational assignment by circular dichroism spectroscopy. *Chem A Eur J*. 2009;15(34):8396-8400.
9. Kosaka T, Iwai S, Inoue Y, Moriuchi T, Mori T, Phys J. *Chem A*. 2018;122:7455-7463.
10. Pescitelli G, Di Bari L, Berova N. Application of electronic circular dichroism in the study of supramolecular systems. *Chem Soc Rev*. 2014;43(15):5211-5233.
11. Ie M, Setsune JI, Eda K, Tsuda A. *Org Chem Front*. 2015;2: 29-33.

12. Hu Y, Paternò GM, Wang X-Y, et al. *J Am Chem Soc*. 2019;141:12797-12803.
13. Carmona M, Rodríguez R, Passarelli V, Lahoz FJ, García-Orduna P, Carmona D. Metal as Source of Chirality in Octahedral Complexes with Tripodal Tetradentate Ligands. *J Am Chem Soc*. 2018;140(3):912-915.
14. Groué A, Tranchier JP, Rager MN, et al. Unique Class of Enantiopure N-Heterocyclic Carbene Half-Sandwich Iridium(III) Complexes with Stable Configurations: Probing Five-Membered versus Six-Membered Iridacycles. *Inorg Chem*. 2019;58(5):2930-2933.
15. Cheng J, Le Saux G, Gao J, et al. *ACS Nano*. 2017;11:3806-3818.
16. George J, Kar S, Anupriya ES, et al. Chiral Plasmons: Au Nanoparticle Assemblies on Thermoresponsive Organic Templates. *ACS Nano*. 2019;13(4):4392-4401.
17. Alonso-Gómez JL, Rivera-Fuentes P, Harada N, Berova N, Diederich F. An enantiomerically pure alleno-acetylenic macrocycle: synthesis and rationalization of its outstanding chiroptical response. *Angew Chem Int Ed*. 2009;48(30):5545-5548.
18. Rivera-Fuentes P, Alonso-Gómez JL, Petrovic AG, et al. Amplification of chirality in monodisperse, enantiopure alleno-acetylenic oligomers. *Angew Chem Int Ed Engl*. 2010;49(12):2247-2250.
19. Míguez-Lago S, Llamas-Saiz AL, MagdalenaCid M, Alonso-Gómez JL. *Chem - A Eur J*. 2015;21:18085-18088.
20. Zubritskaya I, Maccaferri N, Inchausti Ezeiza X, Vavassori P, Dmitriev A. *Nano Lett*. 2018;18:302-307.
21. Ozcelik A, Pereira-Cameselle R, Von Weber A, et al. *Langmuir*. 2018;34:4548-4553.
22. White SJ, Johnson SD, Sellick MA, Bronowska A, Stockley PG, Wälti C. The influence of two-dimensional organization on peptide conformation. *Angew Chem Int Ed*. 2015;54(3):974-978.
23. Zhang Y-Q, Oner MA, Cirera B, et al. Morphological self-assembly of enantiopure allenes for upstanding chiral architectures at interfaces. *Chem Commun*. 2014;50(95):15022-15025.
24. Vericat C, Vela ME, Corthey G, et al. *RSC Adv*. 2014;4:27730-27754.
25. Odermatt S, Alonso-Gómez JL, Seiler P, Cid MM, Diederich F. *Angew Chem Int Ed Engl*. 2005;44:5074-5078.
26. Saragi TPI, Spehr T, Siebert A, Fuhrmann-Lieker T, Salbeck J. Spiro compounds for organic optoelectronics. *Chem Rev*. 2007;107(4):1011-1065.
27. Arias-Coronado VC, Pereira-Cameselle R, Ozcelik A, et al. *Chem – A Eur J*. 2019;25:13496-13499.
28. Poriel C, Rault-Berthelot J, Sicard LJ. New generations of spirobifluorene regioisomers for organic electronics: tuning electronic properties with the substitution pattern. *Chem Commun*. 2019;55(95):14238-14254.
29. Sicard L, Quinton C, Peltier JD, et al. *Chem - A Eur J*. 2017;23:7719-7727.
30. Castro-Fernández S, Cid MM, López CS, Alonso-Gómez JL. *J Phys Chem A*. 2015;119:1747-1753.
31. Castro-Fernández S, Yang R, García AP, et al. Diverse Chiral Scaffolds from Diethynylspiranes: All-Carbon Double Helices and Flexible Shape-Persistent Macrocycles. *Chem A Eur J*. 2017;23(49):11747-11751.
32. Leonard J, Lygo B, Procter G. *in Adv Pract Org Chem*. 2013.
33. Gottlieb HE, Kotlyar V, Nudelman A. NMR Chemical Shifts of Common Laboratory Solvents as Trace Impurities. *J Org Chem*. 1997;62(21):7512-7515.
34. Frisch M. J., Trucks G. W., Schlegel H. B., Scuseria G. E., Robb M. A., Cheeseman J. R., Scalmani G., Barone V., Mennucci B., Petersson G. A., et al., Gaussian Inc., Wallingford 2013.
35. Berova N. *Wiley InterScience (Online service), Comprehensive Chiroptical Spectroscopy. Volume 1, Instrumentation, Methodologies, and Theoretical Simulations*. John Wiley & Sons; 2012.

SUPPORTING INFORMATION

Additional supporting information may be found online in the Supporting Information section at the end of this article.

How to cite this article: Ozcelik A, Peña-Gallego María de los Ángeles, Pereira-Cameselle R, Alonso-Gómez JL. Design and synthesis of chiral spirobifluorenes. *Chirality*. 2020;1–10. https://doi.org/10.1002/chir.23186